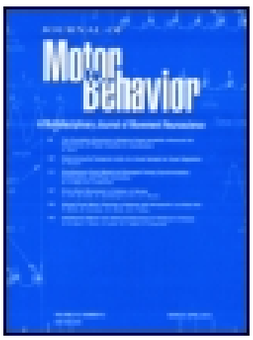

Journal of Motor Behavior

ISSN: (Print) (Online) Journal homepage: https://www.tandfonline.com/loi/vjmb20

Do Tangential Finger Forces Utilize Mechanical Advantage During Moment of Force production?

Junkyung Song , Kitae Kim & Jaebum Park

To cite this article: Junkyung Song , Kitae Kim & Jaebum Park (2020): Do Tangential Finger Forces Utilize Mechanical Advantage During Moment of Force production?, Journal of Motor Behavior, DOI: 10.1080/00222895.2020.1811196

To link to this article: https://doi.org/10.1080/00222895.2020.1811196

Journal of Motor Behavior, 2020

ARTICLE

Do Tangential Finger Forces Utilize Mechanical Advantage During Moment of Force production?

Junkyung Song[1], Kitae Kim[1], Jaebum Park[1,2]

[1]Department of Physical Education, Seoul National University, Seoul, South Korea. [2]Institute of Sport Science, Seoul National University, Seoul, South Korea.

ABSTRACT. This study investigated the beneficial effects of the utilization of mechanical advantage (MA) of finger tangential forces during the moment production. Subjects produced the resistive moment of force against the external torque while the moment arms of the tangential forces were systematically changed. We observed a relatively large contribution to the net moment by the tangential forces with the increased moment arms, whereas the vector sum of normal and tangential forces decreased. The indices of multi-finger coordination for the stabilization of the moment of forces and force direction increased with the moment arms. The current results provide evidence that the utilization of MA is associated with both the efficiency of force production and the stabilization of performance variables.

Keywords: force direction, mechanical advantage, stability, tangential finger force

Introduction

The mechanical advantage (MA) of the human movement system addresses the relationship between an outcome force and a resistive force (Biewener et al., 2004; Demircan et al., 2020). Notably, effectors positioned further away from the axis of rotation have larger MAs for the moment of force production (Shim et al., 2005a; Zatsiorsky et al., 2002a). This implies that a relatively large contribution from effectors with larger MAs (i.e., relatively large shares) would be an efficient and effective way to produce the moment of force. The principle of MA states that the human controller may consider the MA of the effectors for the efficient sharing of activations between involved elements (Zatsiorsky & Latash, 2008). Previous studies have reported that the principle of MA is valid at various levels of the human movement system, including end-effector force generation (Martin et al., 2011; Zatsiorsky et al., 2002b), biting with the teeth (Devlin & Wastell, 1986; Throckmorton & Dean, 1994), and muscle activation (Buchanan et al., 1989; Kuo, 1994; Nichols, 1994; Prilutsky, 2000).

With respect to end-effector force generation and sharing among a redundant set of effectors, the principle of MA is one way to resolve the degrees of freedom problem (Park et al., 2012; Zatsiorsky & Latash, 2008)—not by finding a unique combination of outcome levels of the involved variables (Todorov et al., 2005)—but by conjugating an abundant set of variables (i.e., motor abundance, see Latash, 2012; Reschechtko et al., 2015) based on the rule of organizing sharing and co-variation patterns among the variables. The normal components of finger forces with larger moment arms had larger contributions to the required torque during prismatic grasps using hand digits (Park et al., 2012; Shim et al., 2004; Zatsiorsky et al., 2003b). In particular, the MAs of the index and little fingers are relatively large compared to the middle and ring fingers during prismatic grasping or pressing. This is because of the partially constrained neutral line of the hand, i.e., the line where a zero net moment is observed is likely positioned along the ulnar side of the middle finger (Zatsiorsky & Latash, 2008). Hence, the anatomical structure of the body segment, such as the parallel alignments of fingers, is assumed to be a primary factor for differentiating the MAs of multiple elements related to their sharing strategies when the normal component of finger forces is considered.

A variety of manipulation tasks that use the hand and fingers require the production of appropriate and sufficient shear forces (i.e., tangential forces). A tangential force can be a primary force component that satisfies the task mechanics or carries out everyday activities. For example, the digit tangential forces mainly contribute to the moment production when circular objects are manipulated (Shim & Park, 2007), such as during rotation of a doorknob. Further, load direction affects the sharing patterns of digit tangential forces (Pataky et al., 2004; Slota, Latash, et al., 2012; Slota, Suh, et al., 2012). Of course, the grasping forces (normal force) are necessary to avoid slipping off the hand-held object. However, this does not necessarily mean that the tangential forces passively couple with the normal forces. Thus, the tangential forces can be actively adjusted, given the mechanics necessary for successful performance. Hence, it is plausible that both normal and tangential components of forces are actively controlled, depending on the necessary mechanics of the motor tasks (Latash et al., 2004; Park et al., 2010; Shim & Park, 2007). Generally, the MA of digit tangential forces can be determined by the geometric features of the hand-held object, such as the width of the object being grasped (Adams & Peterson, 1988; Pheasant

Correspondence address: *Jaebum Park, Department of Physical Education & Institute of Sport Science, Seoul National University, #414, 71-1, 1 Gwanak-ro, Gwanak-gu, Seoul 08826, Korea. E-mail: parkpe95@snu.ac.kr*

& O'Neill, 1975; Slota, Latash, et al., 2012; Slota, Suh, et al., 2012). The adjustment of finger tangential forces, by the principle of MA, should cause the redistribution of the finger normal forces. In other words, the local cause-effect adjustments of the finger normal and tangential forces as predicted by the task mechanics are expected, and this phenomenon has been called "chain-effect" (Shim et al., 2003; Zatsiorsky et al., 2002a). Thereby, this leads one to question whether there are similarities between the strategies for the utilization of MA for normal and tangential forces.

Most prior studies have focused mainly on the redistribution of digit force shares relative to changes in MA (Slota, Latash, et al., 2012; Slota, Suh, et al., 2012; Zatsiorsky et al., 2002a), while few studies have explored if the adjustment or redistribution of the force shares, using the principle of MA, benefits performance stability. In this context, "stability" in a redundant human system refers to an ability to maintain or return to an equilibrium of the system by task-specific ways of covaried adjustment and flexible shares of the elements. Consequently, the stable performance in the redundant human system does not require a single solution. Instead, a family of solution would be beneficial for low variability of an important performance variable (PV) (i.e., stable performance), which is well fit to the classical definition of stability. For example, if the hand-held object is unexpectedly perturbed by an external force or torque (Park et al., 2015; Shim et al., 2006), flexible combinations of digit forces (i.e., a family of solution) allow finding ways to maintain the equilibrium such that the mechanical effect of the perturbation is driven by exploring solutions within sub-space of digit forces compatible with the required mechanics. Thus, the stabilization of salient PVs (e.g., net force or torque) is critical for functional actions and could be affected by the sharing and co-variation patterns of redundant elements within the human system.

This study investigated unanswered questions surrounding the manipulation of finger tangential forces, while systematically changing their MAs. Specifically, we examined the beneficial effects of using MA afforded by pressing the index and middle fingers on both mechanical and control aspects of the moment of force production. The MA (i.e., moment arm) of normal forces was uniform, while the MAs of the finger tangential forces were changed by the nonuniform geometries of the external object. We formulated the following hypotheses. The magnitudes of the finger tangential force will increase with the moment arms of the tangential force; this will cause conjoint changes in the finger normal forces (i.e., decrease in the finger normal forces), while the magnitudes of the finger normal forces will always be larger than those of finger tangential forces for the slippage prevention (Hypothesis 1). Since both finger normal and tangential forces contributed to the moment production in the current task, we explored the changes in the stability indices of the moments of finger normal and tangential forces, separately. We expected the non-parallel changes of the stabilization of two components of moment production such that the indices to stabilize the moment of tangential force will increase with the increment of moment arms, while the stability indices for the moment of normal force will decrease (Hypothesis 2). Further, we explored the combined effects of finger normal and tangential forces. We hypothesized that the increased MAs of tangential forces would be associated with increments of the stability indices that are related to the magnitude of the net moment and force direction (i.e., the direction of force vector) (Hypothesis 3).

Materials and methods

Participants

Twenty young subjects including six females (age: 28.43 ± 4.94 years; weight: 68.62 ± 12.14 kg; height: 171.25 ± 5.67 cm; mean ± SD) participated in this study. The hand dominance of the subjects was determined by the scores of the Edinburg handedness inventory (Oldfield, 1971). The average score across the subjects was larger than 80 (83.3 ± 13.1, mean ± SD across the subjects), which confirmed that all the participants were considered right-handers. No participants had any sign and history of neuropathies or traumas to their upper extremities. Prior to the experiment, the experimental procedures of the study were explained to the participants, and they signed a consent form. The consent form indicated the procedures and potential risks involved during the experiment in accordance with the ethical standards set by the Institutional Review Board of Seoul National University (IRB No. 1907/003-015).

Apparatus

Two multi-component force/torque transducers (Nano-17, ATI Industrial Automation, Garner, NC) being attached to the customized flat steel-frame (14×5 cm) were used to measure individual finger forces in both normal (z-axis) and tangent directions (y-axis) (Figure 1(A)). The two transducers were aligned in the x-y plane, i.e., horizontal plane, and there were two slits along the x-axis to attach the transducers. The surfaces of the transducers were covered with 100-grit sandpaper (friction coefficient: $1.40 \sim 1.52$) to provide sufficient friction between the fingertips and contact surface of the corresponding transducers (Park et al., 2012; Shim & Park, 2007; Zatsiorsky et al., 2003a). The experimental frame was designed such that it allowed movement in the rotation about the x-axis only (Figure 1(A)). In other words,

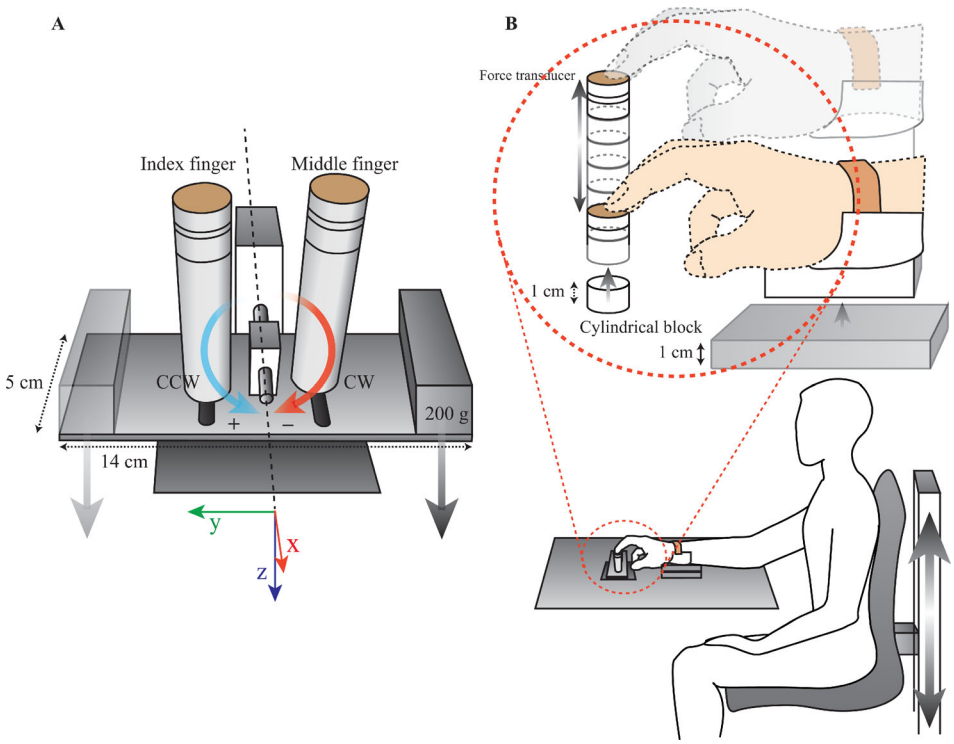

FIGURE 1. Experimental setup. (A) Two six-dimensional force/torque transducers were mounted on steel-frame that could be rotated along the *x*-axis by the production of finger forces. The 0.2 kg load was attached to the frame in order to produce external torque in clockwise (–) or counter-clockwise (+) directions. (B) The cylindrical spacers were used to adjust the height of the transducers, and the height of the forearm brace was also adjusted accordingly to ensure the constant wrist and finger configuration during the tasks.

the frame with the transducers was not mechanically fixed, but the frame could rotate about a shaft passing through the center of the frame. The friction during the rotation was supposed to be minimal as the contact surface of the shaft was small and an oil grease was injected into the hole where the shaft passed.

A set of cylindrical spacers (Figure 1(B)) whose diameters were identical to those of the transducers (17 mm diameter) were employed to implement changes of the moment arms of the finger tangential forces. The height of each spacer was 1 cm and different sets of the spacers allowed changing the moment arms from 0 cm (no spacer) to 10 cm (10 spacers) at 1 cm interval. Note that the position of the center of rotation was above the steel-frame by the height of the transducers; thus, the moment arm of the finger tangential force with no spacer was supposed to be zero. A 0.2 kg load was mounted and fixed on either right or left end of the frame in order to create external torque in the clockwise (CW) and counter-clockwise (CCW) directions (Figure 1(A)). In addition, a bubble level was placed on the other side of the load, allowing participants to monitor the angular position of the lever. The force signals recorded from the sensors were digitized with an analog-to-digital converter (Gen5, AMTI, Watertown, MA).

The rotation of the frame with the transducers was constrained to the *x*-axis, therefore, the force components along the y- and *z*-axis were supposed to contribute to the production of the moment of force about the *x*-axis. The distance between the slits was 4 cm, and the center of rotation was positioned midway between the two transducers. Thus, the magnitude of the moment arm of the normal forces (i.e., force component along the *z*-axis) for the two fingers was fixed at 2 cm.

Experimental Procedures

The subjects visited the laboratory for two consecutive days. On the first day, the subjects had at least 30 min orientation session to become familiar with the experimental setup by performing practice trials. We assumed that 30 min practice was enough time for the subjects to become familiar with the tasks, and the learning was possibly completed by the practice session (i.e., no learning effect during the experiment). Further, the subjects performed half of the whole tasks on the first day. On

the second day, the subjects had a short practice session and performed the rest of the trials. Note that the data from practice trials were not considered for the analysis, and the number of rejected trials by failing the task during actual data acquisition was less than one per condition for each subject. The subjects sat in a height-adjustable chair and were instructed to place the index and middle fingertips of the right on the corresponding transducers (Figure 1(B)) and positioned their right forearm on a wrist-forearm brace (semi-circular plastic cylinder) that was fixed to a table. Non-involved digits, including the thumb, ring, and little finger were flexed naturally while not contacting frame and transducers; therefore, non-involved digits had no mechanical effect on the frame during the tasks. The forearm was held stationary with Velcro straps to prevent excessive forearm and wrist movement during the tasks. Before the initiation of each trial, the subjects placed the distal phalange of each digit on the center of the corresponding transducer, and each trial lasted 10 s. Once the trial started, the subjects were instructed to maintain the rotational equilibrium with minimal efforts (i.e., the avoidance of excessive pressing) for at least 5 s. A bubble level provided visual feedback on the rotation of the frame. Note that there was a single mechanical constraint that was "zero net moment by producing normal and tangential forces by the two fingers".

There were 11 conditions of the moment arms of the tangential finger forces, which were given by adjusting the number of the spacers (Figure 1). The height of each spacer was 1 cm and the moment arm conditions were given from 0 (no spacer) to 10 cm (10 spacers) at 1 cm interval. As the condition of the moment arm changed, the heights of both chair and forearm brace were adjusted accordingly to configure the constant forearm and finger geometry during the tasks (Figure 1(B)), which avoided possible changes in the peripheral properties of the flexor muscles (i.e., spring-like properties of the muscles). Further, two external torques, which required the subject to produce the CW and CCW moments, were given at each moment arm condition (Figure 1(A)). For each combination of moment arm and external torque condition, the subject performed 20 consecutive trials; therefore, a total of 440 trials (11-moment arm conditions × 2 external torque conditions × 20 trials) were performed for each subject. The conditions were given in a block randomized order across the subjects, and each combination was presented as a block of 20 trials.

All force signals were set to zero before each trial began and the sampling frequency of finger force data was set at 100 Hz. A rest interval was given to the participant between trials and moment arm conditions to minimize fatigue, and no participant reported fatigue. The rest interval between trials and between moment arm conditions were 20 s and 5 min, respectively.

Data Analysis

The recorded finger force data were analyzed offline using customized code written in MATLAB (MathWorks Inc., Natick, MA). The fourth-order, zero-lag Butterworth filter with a 10 Hz cutoff was applied to the raw force data. The filtered finger force data from each trial were averaged over 1 s in the middle of 5 s data where steady-state values of net moment of force (i.e., zero net torque) were observed.

Mechanical Constraint of the Task

The mechanical constraint in this study was limited to the finger forces in the y-z plane, and the force component of the y- (i.e., tangential force) and z- (i.e., normal force) contributed to the resultant moment of force (M^{RES}) production. Hence, the following task constraint (torque constraint) was supposed to be satisfied by producing appropriate forces with the index and middle fingers (Equation (1)).

$$\begin{aligned} M_x^{\mathrm{RES}}(t) &= \left[d_y^I \cdot F_z^I(t) - \ d_z^{I,j} \cdot F_{\mathrm{y}}^I(t)\right] \\ &\quad + [d_y^M \cdot F_z^M(t) - \ d_z^{M,j} \cdot F_y^M(t)] \\ &= \ -Tq^k \end{aligned} \tag{1}$$

where j stands for the moment arm condition (i.e., $j = \{0, 1, \cdots 10\}$). Note that the moment arms of the finger normal forces (d_y) were constant, while the moment arms of the finger tangential forces (d_z) were varied depending on the experimental conditions. $k = \{\mathrm{CW}, \mathrm{CCW}\}$; M, F, and d stand for the moment of force, force, and moment arm, respectively; subscript x, y, and z refer to the x-, y-, and z-axis; superscript I and M indicate the index and middle finger. F_z^i and F_y^i coincide with the finger normal (F_N^i) and tangential forces (F_T^i), respectively, where $i = \{$index (I), middle (M), resultant (RES)$\}$. We computed the direction (i.e., arctangent of the ratio of tangential to normal force) of force vectors of the index (F_{DIR}^I) and middle finger (F_{DIR}^M) separately. The resultant moment of force (M^{RES}) was decomposed into the moment by the normal (M_N^{RES}) and tangential force (M_T^{RES}). The M^{RES} was further classified into moment agonist (M_{AGO}) and antagonist (M_{ANT}) with respect to the moment in the required direction against the external torque (Tq), and the ratio of the magnitudes of the agonist–antagonist moment ($M_{AGO/ANT}$) was computed. All these mechanical variables were calculated for each trial and further averaged across multiple trials and then across the subjects for each condition separately. Lastly, we calculated the safety margin (SM), which is the quantification of the difference between the magnitudes of measured normal force and the minimum

requirement of the normal force for the slippage prevention (Flanagan & Wing, 1993; Johansson & Westling, 1984). In each moment arm condition, the SMs of the index and middle finger were calculated separately using Equation (2).

$$SM^i = \frac{\left(F_N^i - \left|F_T^i\right|/\mu\right)}{F_N^i} \quad (2)$$

where i is an individual finger, and F_N and F_T stand for the normal and the tangential finger forces, respectively. μ was set at 1.4 as the friction coefficient between the finger pad and the sandpaper interface.

Principal Component Analysis

A principal component analysis (PCA) with a variance maximizing rotation (i.e., varimax rotation) was performed to identify the significant number of linear combinations (PCs) among the four component of finger forces including the normal and tangential forces of the index and middle fingers (F_N^I, F_T^I, F_N^M, and F_T^M) over 20 observations for each condition and subject, separately. The Kaiser Criterion, i.e., extracted PCs should be the eigenvectors whose eigenvalues are larger than 1, was employed to extract the significant PCs and loading coefficients in the PCs (Kaiser, 1960).

Coordination Index of Multi-components of Finger Forces

The force data were analyzed within the framework of the uncontrolled manifold (UCM) hypothesis (Latash et al., 2007; Scholz et al., 2002; Scholz & Schoner, 1999). This computational method has been used to quantify the patterns of co-variation among the involved elements (e.g., finger forces in this study) for the stabilization of important PVs including mechanically constrained (e.g., the moment of force) and hypothetical variables (e.g., force direction). The hypothetical PVs refer to the variables that were not constrained but assumed to be stabilized due to potential importance. In the current study, we tested the stabilizations of four PVs, including 1) resultant moment force (M^{RES}), 2) resultant moment of normal force (M_N^{RES}), 3) resultant moment of tangential force (M_T^{RES}), and 4) direction of force vector (F_{DIR}), separately. The changes in the values of each PV can be written as a function of the force vector, Δf as follows (Equation (3)).

$$\Delta PV = J \cdot \Delta f^{\mathrm{T}} \quad (3)$$

where J is the Jacobian that links infinitesimal changes in finger forces with changes in the PVs, and superscript T is a sign of transpose. The Jacobians for the M^{RES}, M_N^{RES}, and M_T^{RES}-related analyses were $[d^I_y\ d^I_z\ d^M_y\ d^M_z]$, $[d^I_y\ d^M_y]$, and $[d^I_z\ d^M_z]$, respectively. For the force direction (F_{DIR})-related analysis, the Jacobian was configured as $[1/\Sigma F_N\ -\Sigma F_T/(\Sigma F_N)^2\ 1/\Sigma F_N\ -\Sigma F_T/(\Sigma F_N)^2]$.

Briefly, two manifolds were found by computing the null space and its orthogonal space of the Jacobian that spanned by linearly approximated basis vectors. Then, two components of variances within two separated manifolds, V_{UCM} and V_{ORT}, were computed across the 20 trials for each condition and subject. The UCM was defined as an orthogonal set of the unit vectors in the finger forces space where the changes in finger force combinations did not change the net outcomes. The other subspace (ORT) was the orthogonal vector to the UCM. The synergy index (ΔV) was computed as the difference between V_{UCM} and V_{ORT}, which was normalized by the total variance (V_{TOT}) (Equation (4)). The two components of variances were further normalized by the degrees of freedom of the corresponding subspace, which allowed making comparable indices across two subspaces that were observed in different dimensions.

$$\Delta V = \frac{V_{UCM}/DOF_{UCM} - V_{ORT}/DOF_{ORT}}{V_{TOT}/DOF_{TOT}} \quad (4)$$

In addition, the ΔVs and SMs were log-transformed for the statistical comparison between the conditions using the Fischer transformation applied for the computational boundaries such that -4 to $+1.33$ for M^{RES} & F_{DIR}-related analyses, -2 to 2 for the M_N^{RES} & M_T^{RES}-related analyses, and 0–1 for the SM.

Statistics

A standard description of parametric statistics was used, and the data are presented as means and standard error. Repeated-measured ANOVAs with the factors of *Direction* (two levels: CW and CCW), *Moment Arm* (11 levels: $0 \sim 10$ cm at 1 m interval), *Force component* (two levels: normal and tangential component), *Finger* (two levels: index and middle), and *Variance* (two levels: UCM and ORT) were performed to test how the quantified variables were affected by a set of factors. The factors were selected for particular comparisons to test the hypotheses.

To explore the effect of the changes in the moment arms on the difference in the mechanical variables of the normal and tangential component, two-way repeated-measured ANOVAs were done separately on the finger forces (F) and the moment of finger forces (M) with factors *Force component* and *Moment Arm* (Hypothesis 1). In addition, auxiliary ANOVAs were performed on the force direction (F_{DIR}) and SM with factors *Finger* and *Moment Arm*.

Two-way repeated-measured ANOVAs with factors *Force component* and *Moment Arm* were performed on the synergy indices (ΔV) in the CW and CCW condition, separately. Further, we explored the effect of *Moment Arm* on the difference in the variances within the two subspaces (UCM and ORT) with the factors *Variance* and *Moment Arm* (Hypothesis 2).

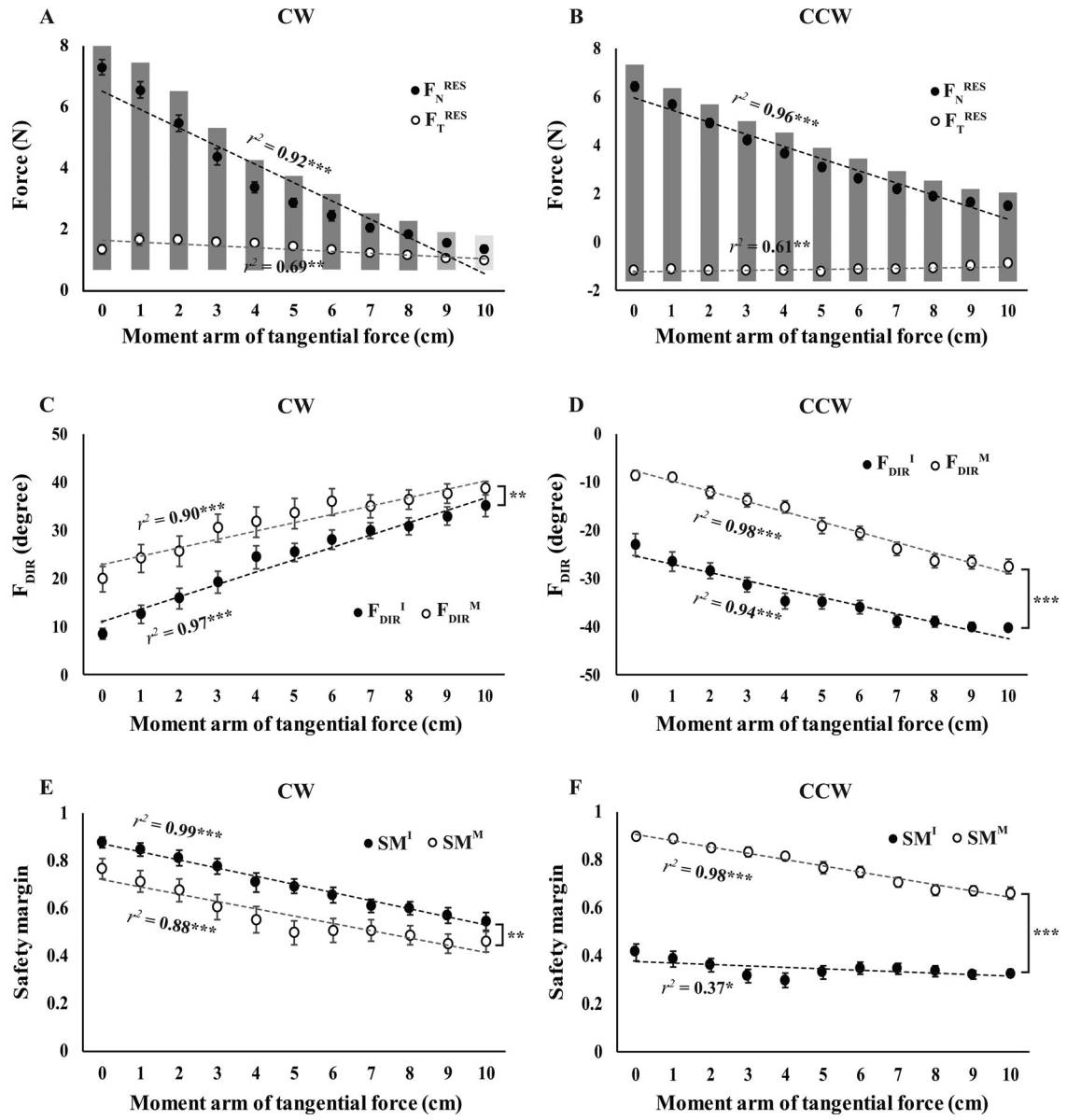

FIGURE 2. Changes in the resultant normal force (F_N^{RES}, filled circles) and tangential force (F_T^{RES}, open circles) with the moment arms conditions for **(A)** CW and **(B)** CCW condition. Changes in F_{DIR}^{I} (filled circles) and F_{DIR}^{M} (open circles) with the moment arms for **(C)** CW and **(D)** CCW condition. Changes in SM^I (filled circles) and SM^M (open circles) with the moment arms for **(E)** CW and **(F)** CCW condition. Values are means ± standard errors across subjects. The dotted lines with the coefficients of determination (r^2) represent the significant changes of the variables over the moment arm conditions from the regression analyses. Triple asterisks (***) indicate $p < .001$; double asterisks (**) indicate $p < .01$; single asterisks (*) indicate $p < .05$ for the regression analyses and main effects of the ANOVAs. *Vertical gray bars* indicate significant differences of post hoc comparisons; dark gray indicates $p < .001$; medium gray indicates $p < .01$; light gray indicates $p < .05$.

To compare the synergy indices of the net moment (ΔV_M^{RES}) and force direction (ΔV_F^{DIR}) across *Moment Arm* and *Direction*, two-way repeated-measured ANOVAs were done (Hypothesis 3). Also, a similar ANOVA was performed on the ratio of agonist and antagonist moment ($M_{AGO/ANT}$).

Mauchly's sphericity test was used to confirm the assumptions of sphericity, and the sphericity violations were corrected by the Greenhouse–Geisser estimation. Tukey's honestly significant difference tests and pairwise comparisons were performed to explore significant effects. In addition, the regression analyses as auxiliary

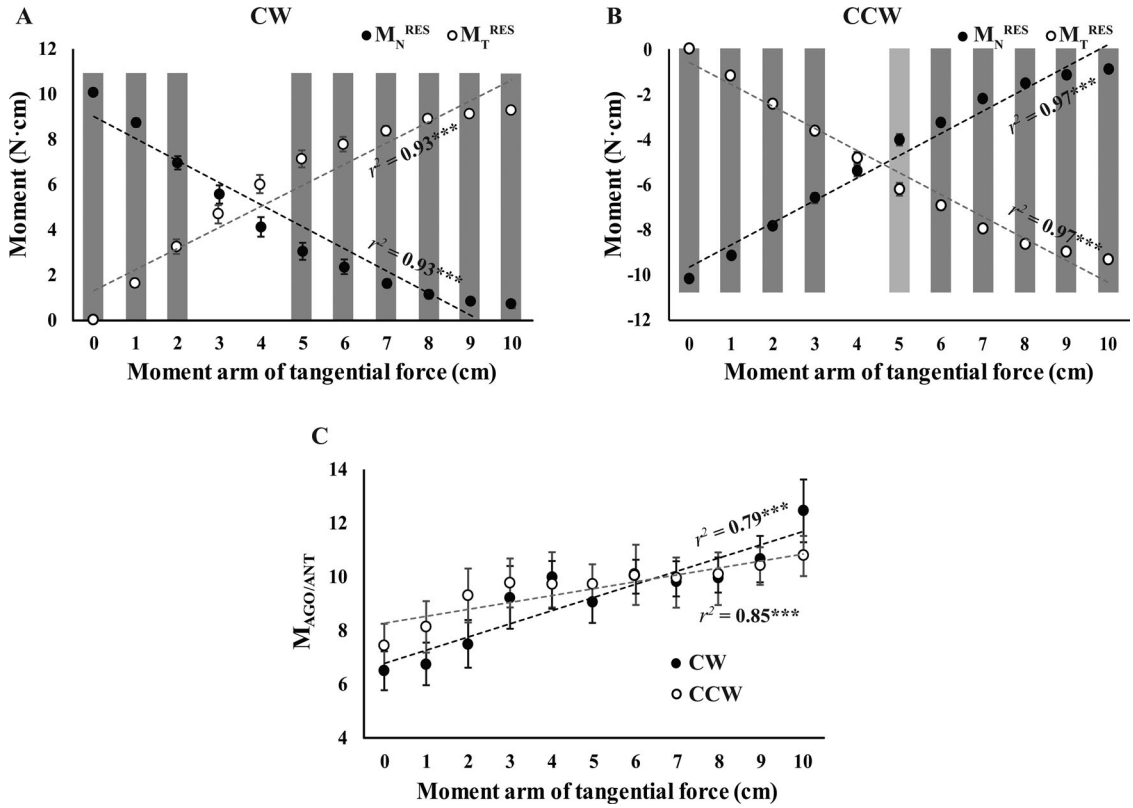

FIGURE 3. Changes in the resultant moment of normal force (M_N^{RES}, filled circles) and tangential force (M_T^{RES}, open circles) for **(A)** CW and **(B)** CCW condition. **(C)** The ratio of the magnitudes of M_{AGO} to M_{ANT} ($M_{AGO}/_{ANT}$) for CW (filled circles) and CCW (open circles) condition. Regression lines are shown with the coefficients of determination (r^2). The average data across subjects are presented with standard error bars. Triple asterisks (***) indicate $p < .001$. *Vertical gray bars* indicate significant differences of post hoc comparisons; dark gray indicates $p < .001$; medium gray indicates $p < .01$.

tests were performed to identify the patterns of the significant changes (e.g., linear increment or decrement) in particular dependent variables over the moment arm conditions. Lastly, PCA was performed to observe the configurations of the dataset and their dimension reduction (for more details, see *Data Analysis* section). The effect size, the partial eta-squared (ηp^2), was calculated for all presented results. We conducted all statistical analyses using SPSS 24.0 (IBM, Armonk, NY), and the level of significance was set at $p<.05$.

Results

Changes in Finger Force Production

In general, the magnitudes of resultant normal finger force (F_N^{RES}) were larger than the resultant finger tangential force (F_T^{RES}) for all experimental conditions. Also, the magnitudes of F_N^{RES} and F_T^{RES} decreased with the magnitudes of the moment arms of the finger tangential forces during both the CW and CCW conditions. Further, the decrements in the magnitudes of the two force components were not parallel showing a stiffer decrement in F_N^{RES} compared to F_T^{RES} (Figure 2(A,B)), which was partially in line with Hypothesis 1. These results were supported by two-way repeated-measures ANOVAs with factors *Force component* (two levels: normal and tangential component) and *Moment Arm* (11 levels: $0 \sim 10$ cm at 1 cm interval) separately on each torque direction. There were significant main effects of *Force component* (CW: $F_{[1,19]}=152.94$, $p< .001$, $\eta p^2=0.89$; CCW: $F_{[1,19]}=1540.02$, $p< .001$, $\eta p^2=0.99$) and *Moment Arm* (CW: $F_{[2.57,48.88]}=255.69$, $p< .001$, $\eta p^2=0.93$; CCW: $F_{[3.36,63.76]}=249.12$, $p< .001$, $\eta p^2=0.93$) with significant factor interaction of *Force component* × *Moment arm* (CW: $F_{[3.03,57.60]}=109.71$, $p< .001$, $\eta p^2=0.85$; CCW: $F_{[3.08,58.53]}=395.95$, $p< .001$, $\eta p^2=0.95$). The significant factor interactions reflected the fact that the magnitudes of F_N^{RES} were significantly larger than those of F_T^{RES} for the all moment arm conditions, which was confirmed by post hoc comparisons ($p< .05$). In addition, the regression analyses further

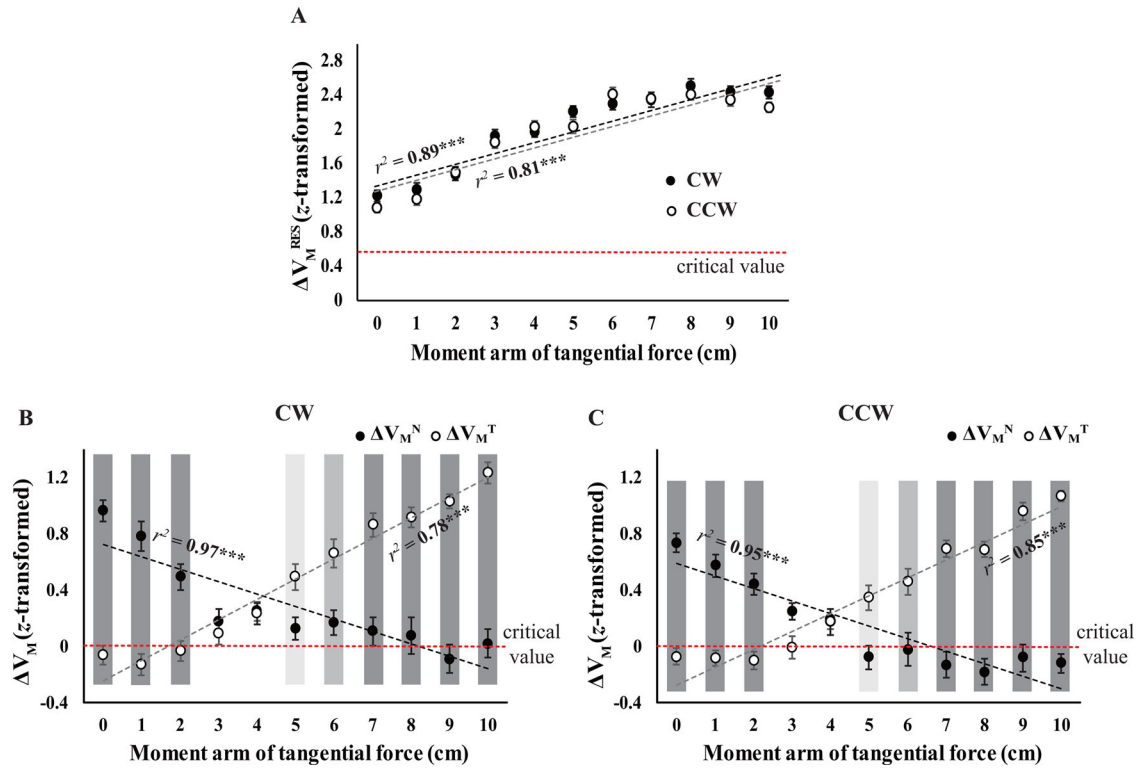

FIGURE 4. Changes in *z*-transformed synergy indices for the stabilization of **(A)** the resultant moment of force (ΔV_M^{RES}), the moment of normal force (ΔV_M^N), and the moment of tangential force (ΔV_M^T) for (**B**) CW and (**C**) CCW condition. Regression lines are shown with the coefficients of determination (r^2). The dashed horizontal lines in red color indicate the critical values of ΔV for the existence of the synergy. The average data across subjects are presented with standard error bars. Triple asterisks (***) indicate $p < .001$. *Vertical gray bars* indicate significant differences of post hoc comparisons; dark gray indicates $p < .001$; medium gray indicates $p < .01$; light gray indicates $p < .05$.

confirmed that the significant decreases in F_N^{RES} and F_T^{RES} over the moment arms were best fit by a linear model for all conditions ($p < .01$).

The signs of the force directions (F_{DIR}) for the CW (Figure 2(C)) and CCW (Figure 2(D)) conditions were positive and negative respectively throughout all the moment arm conditions and no sign differences between the directions of two fingers forces. F_{DIR} for both the index (F_{DIR}^I) and middle fingers (F_{DIR}^M) increased in the CW condition, while F_{DIR}^I and F_{DIR}^M decreased in the CCW condition over the moment arm conditions. Further, the F_{DIR}^M were larger than F_{DIR}^I for both the CW and CCW conditions (i.e., more positive for the CW, and less negative for the CCW for the F_{DIR}^M). These findings were supported by two-way repeated-measures ANOVAs with factors *Finger* and *Moment Arm*, which showed significant main effects of *Finger* (CW: $F_{[1,19]}=10.98$, $p= .004$, $\eta p^2=0.37$; CCW: $F_{[1,19]}=129.35$, $p< .001$, $\eta p^2=0.87$) and *Moment Arm* (CW: $F_{[3.69,70.03]}=42.41$, $p< .001$, $\eta p^2=0.69$; CCW: $F_{[3.54,67.27]}=74.96$, $p< .001$, $\eta p^2=0.80$) without factor interactions. Significant increment and decrement of the F_{DIR} for the CW and CCW conditions over the moment arms were best fit by a linear equation for both F_{DIR}^I and F_{DIR}^M ($p < .001$).

The SM of the index (SM^I) and middle fingers (SM^M) were decreased as the moment arms increased in both the CW and CCW conditions. The SM of which normal force produced the agonist moment was larger than the SM of the other finger (e.g., $SM^I > SM^M$ for the CW) (Figure 2(E,F)). Two-way repeated-measures ANOVAs with factors *Finger* and *Moment arm* performed separately showed significant main effects of *Finger* (CW: $F_{[1,19]}=12.15$, $p=.002$, $\eta p^2=0.39$; CCW: $F_{[1,19]}=122.40$, $p< .001$, $\eta p^2=0.87$) and *Moment arm* (CW: $F_{[3.58,67.94]}=36.97$, $p< .001$, $\eta p^2=0.66$; CCW: $F_{[4.17,75.07]}=66.22$, $p< .001$, $\eta p^2= 0.79$) without factor interactions.

Changes in Moment of Force Production

The magnitudes of the resultant moment of force (M^{RES}) for the static equilibrium did not show statistical

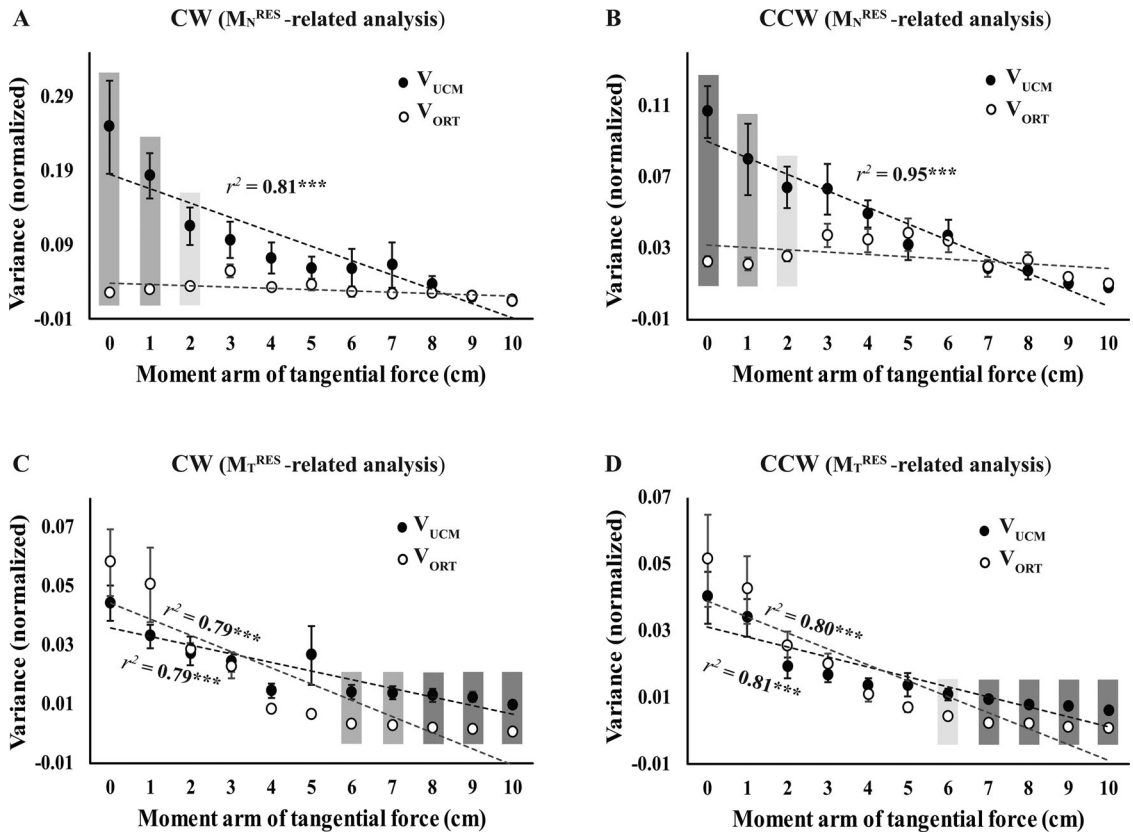

FIGURE 5. Two components of variance, V_{UCM} (filled circles) and V_{ORT} (open circles), for the resultant moment of normal force (M_N^{RES})-related analysis for **(A)** CW and **(B)** CCW condition, and for the resultant moment of tangential force (M_T^{RES})-related analysis for **(C)** CW and **(D)** CCW condition. Values are means ± standard errors across subjects. Regression lines are shown with the coefficients of determination (r^2). Triple asterisks (***) indicate $p < .001$. *Vertical gray bars* indicate significant differences of post hoc comparisons; dark gray indicates $p < .001$; medium gray indicates $p < .01$; light gray indicates $p < .05$.

differences between the experimental conditions ($p > .05$, not shown in Figure). The magnitudes of the resultant moment by the normal force (M_N^{RES}) decreased, while the resultant moment by the tangential force (M_T^{RES}) increased over the moment arm conditions for both the CW and CCW conditions (Figure 3(A,B)), which further supported the Hypothesis 1. Two-way repeated-measures ANOVAs that performed with factors *Force Component* and *Moment Arm* confirmed the significant main effects of *Force Component* (CW: $F_{[1,19]}=17.47$, $p = .001$, $\eta p^2=0.48$; CCW: $F_{[1,19]}=9.63$, $p = .006$, $\eta p^2=0.34$) with significant *Force component* × *Moment Arm* (CW: $F_{[2.63,50.04]}=304.93$, $p < .001$, $\eta p^2=0.94$; CCW: $F_{[2.69,51.15]}=614.51$, $p < .001$, $\eta p^2=0.97$). The significant factor interactions reflected the fact that the patterns of changes in the M_N^{RES} and M_T^{RES} were opposite to each other. The *post hoc* pairwise comparison confirmed that the significant differences between M_N^{RES} and M_T^{RES} were shown in most of the moment arm conditions except in 3 and 4 cm for the CW and 4 cm for the CCW direction. Further, the regression analyses confirmed that the significant changes in each of M_N^{RES} (i.e., decrement) and M_T^{RES} (i.e., increment) over the moment arms were described best by linear models ($p < .001$).

The ratio of the magnitudes of agonist to antagonist moment ($M_{AGO/ANT}$) increased with the magnitudes of moment arms, and there was no significant difference on $M_{AGO/ANT}$ between the CW and CCW conditions (Figure 3(C)), which confirmed by a significant main effect of *Moment Arm* ($F_{[3.41,54.56]}=9.10$, $p < .001$, $\eta p^2=0.36$) without factor interaction. Significant increments of the $M_{AGO/ANT}$ over the moment arms for all the torque conditions were the best fit by linear equations ($p < 0.001$).

Coordination Indices

Moment Stabilization Hypothesis

ΔV_M^{RES}, which represents the stability index for the stabilization of net moment, increased linearly with the moment arms ($F_{[10,190]}=111.48$, $p < .001$, $\eta p^2=0.85$,

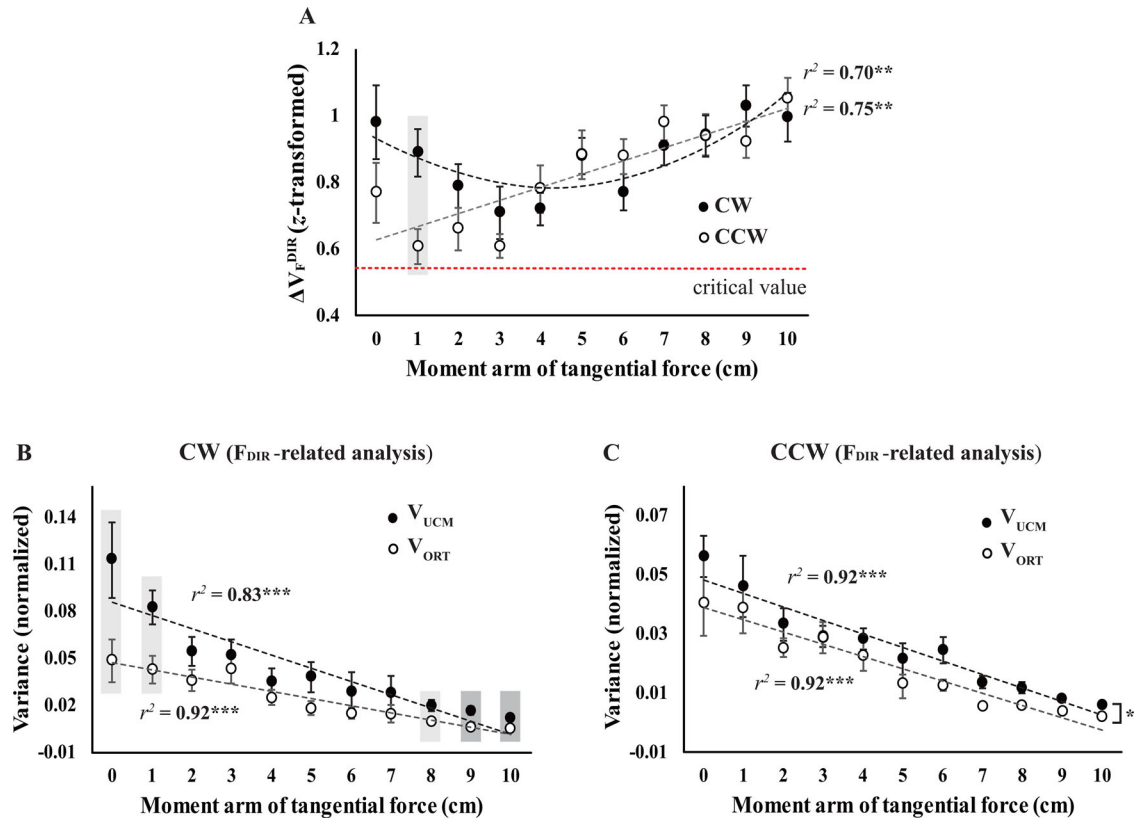

FIGURE 6. **(A)** Changes in *z*-transformed synergy indices for the stabilization of the force direction (ΔV_F^{DIR}) for CW (filled circles) and CCW (open circles) condition. The dashed horizontal lines in red color indicate the critical values of ΔV for the existence of the synergy. Two components of variance, V_{UCM} (filled circles) and V_{ORT} (open circles) for the force direction-related analysis for **(B)** CW and **(C)** CCW condition, are presented. Values are means ± standard errors across subjects. Regression lines are shown with the coefficients of determination (r^2). Triple asterisks (***) indicate $p < .001$; double asterisks (**) indicate $p < .01$; single asterisks (*) indicate $p < .05$ for the regression analyses and the main effects of ANOVAs. *Vertical gray bars* indicate significant differences of post hoc comparisons; medium gray indicates $p < .01$; light gray indicates $p < .05$.

Figure 4(A)) with no significant difference between the CW and CCW conditions (Hypothesis 3). We further compared two components of variances, V_{UCM} and V_{ORT}, which showed that the V_{UCM} was always larger than the V_{ORT} for all experimental conditions ($p < .001$, not shown in Figure). Both variances decreased with the moment arms ($p < .001$), while relatively large decrements in the V_{UCM} compared to V_{ORT} that were confirmed by significant *Variance* × *Moment Arm* (CW: $F_{[2.82,53.56]}=8.03$, $p < .001$, $\eta p^2=0.62$; CCW: $F_{[3.45,65.61]}=7.16$, $p < .001$, $\eta p^2 =0.27$).

There were opposite changes in the synergy indices for the stabilization of moment of normal force (ΔV_M^N) and tangential forces (ΔV_M^T), which was commonly observed in both CW and CCW conditions (Figure 4(A)). That was the ΔV_M^N decreased, while the ΔV_M^T increased with the moment arms (Figure 4(B,C)), which supported the Hypothesis 2. These results were supported by two-way repeated-measures ANOVAs with factors *Force component* and *Moment Arm* separately on torque directions, which showed significant main effects of *Force component* (CW: $F_{[1,19]}=9.59$, $p= .006$, $\eta p^2=0.34$; CCW: $F_{[1,19]}=20.34$, $p<.001$, $\eta p^2=0.52$) and *Moment Arm* (CW: $F_{[5.34,101.47]}=6.27$, $p < .001$, $\eta p^2=0.25$; CCW: $F_{[10,190]}=4.02$, $p < .001$, $\eta p^2=0.18$) with significant *Force component* × *Moment Arm* (CW: $F_{[10,190]}=83.31$, $p < .001$, $\eta p^2=0.81$; CCW: $F_{[6.10,115.96]}=75.46$, $p < .001$, $\eta p^2=0.80$). As a result of post hoc pairwise comparison, significant differences between ΔV_M^N and ΔV_M^T were observed in overall moment arm conditions except in 3 and 4 cm for both CW and CCW condition ($p < .05$). Further, the significant decrements and increments in ΔV_M^N and ΔV_M^T over the moment arms were well described by a linear regression ($p < .001$).

For the moment of normal force (M_N)-related analysis, V_{UCM} decreased over the moment arm conditions, while no significant changes in V_{ORT}. The V_{UCM} was larger

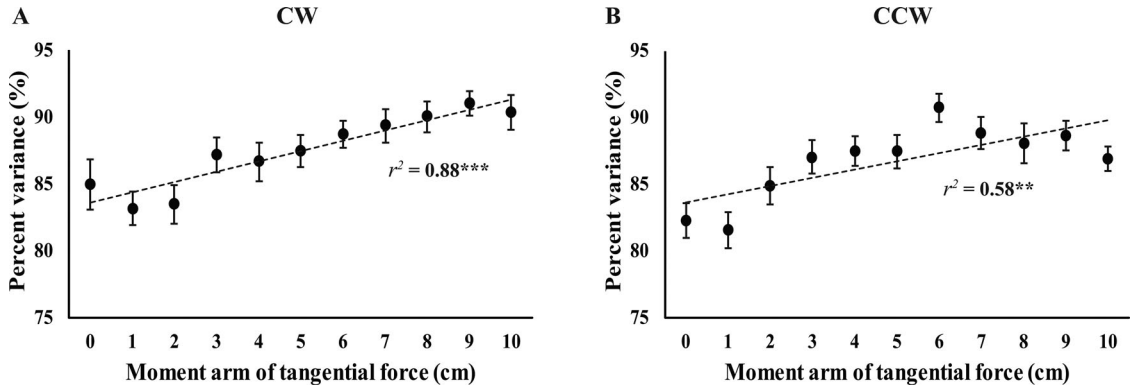

FIGURE 7. Changes in the percent variance explained by significant principal components (PCs) for **(A)** CW and **(B)** CCW condition. The average data across the subjects are shown with standard error bars. Regression lines are shown with the coefficients of determination (r^2). Triple asterisks (***) indicate $p < .001$; double asterisks (**) indicate $p < .01$.

than V_{ORT} at relatively small moment arm conditions (e.g., $0 \sim 2$ cm), which were confirmed by significant factor interactions of *Variance* × *Moment Arm* (CW: $F_{[2.21,41.98]} = 10.14$, $p < .001$, $\eta p^2 = 0.35$; CCW: $F_{[3.55,67.37]} = 12.66$, $p < .001$, $\eta p^2 = 0.40$) (Figure 5(A,B)). Similarly, for the moment of tangential force (M_T)-related analysis, both V_{UCM} and V_{ORT} decreased with the moment arm conditions ($p < .05$). The statistical differences between V_{UCM} and V_{ORT} were observed only at $6 \sim 10$ cm moment arm condition, which was confirmed by significant factor interactions of *Variance* × *Moment Arm* (CW: $F_{[2.98,56.57]} = 3.57$, $p < .05$, $\eta p^2 = 0.35$; CCW: $F_{[10,190]} = 2.05$, $p < .05$, $\eta p^2 = 0.40$) (Figure 5(C,D)).

Force-direction Stabilization Hypothesis

The synergy indices to stabilize the direction of resultant force (ΔV_F^{DIR}) varied depending on moment arm conditions. Generally, the ΔV_F^{DIR} decreased slightly and then increased with moment arms for the CW condition, and the ΔV_F^{DIR} in the CCW condition increased according to increasing moment arms (Hypothesis 3). The significant difference on ΔV_F^{DIR} between the CW and CCW condition was observed only at 1 cm condition (Figure 6(A)). Two-way repeated-measures ANOVA with factors *Direction* and *Moment Arm* confirmed these findings, which showed significant main effects of *Moment Arm* ($F_{[4.56,77.50]} = 7.00$, $p < .001$, $\eta p^2 = 0.30$) with significant factor interaction of *Direction* × *Moment Arm* ($F_{[10,170]} = 2.76$, $p = .003$, $\eta p^2 = 0.14$). Further, the changes in ΔV_F^{DIR} for the CW condition was best fitted by a quadratic function ($p = .008$), while it was sufficiently described by a linear equation for the CCW condition ($p = .001$). The V_{UCM} and V_{ORT} showed a gradually decreasing pattern with increasing moment arm in both the CW and CCW conditions. In the case of the CW condition, the magnitudes of V_{UCM} were larger than V_{ORT} in 0, 1, 8, 9, and 10 cm of the moment arm conditions ($p < .05$) (Figure 6(B)). For the CCW, the V_{UCM} always larger than V_{ORT} in all moment arm conditions ($p < .05$) (Figure 6(C)).

Dimension Reduction by Principal Component Analysis (PCA)

The PCA was performed on the sets of 20 observations for each subject and condition. Generally, the number of significant PCs was two, which accounted for more than 85% of total variance for all subjects and conditions ($87.50 \pm 2.72\%$ for the CW and $86.72 \pm 2.77\%$ for the CCW; mean ± standard deviation across all subjects and moment arm conditions), which describes that the experimental observations from the multiple trials were confined to a two-dimensional hyperplane in the four-dimensional force space. In addition, the percent variances explained by the first two PCs increased significantly with the magnitudes of moment arm for both the CW and CCW conditions ($p < .05$) (Figure 7).

The loadings for a set of variables in PC1 and PC2 were calculated for each moment arm condition (Table 1), and the patterns of loadings for the variables within two PCs showed systematic changes with the magnitudes of moment arms. For the relatively lower moment arm conditions (e.g., $0 \sim 2$ cm conditions), the normal forces of two fingers (F_N^I and F_N^M) had large loadings ($|\text{loading}| > 0.8$) with the same sign in the PC1, whereas the tangential forces of two fingers (F_T^I and F_T^M) had large loadings in the PC2. For the mid-range of moment arm conditions (e.g., $3 \sim 5$ cm conditions), the normal and tangential forces of each finger were observed in the same PC. The two force components of the index and

TABLE 1. Loadings of principal components (PC1 and PC2) of all finger force components in each moment arm and torque direction condition.

Moment arm (cm)	Variable	CW PC1	CW PC2	CCW PC1	CCW PC2	Moment arm (cm)	CW PC1	CW PC2	CCW PC1	CCW PC2
0	F_N^I	**0.97**	−0.07	**0.91**	0.21	**6**	0.37	**0.90**	**0.86**	0.14
	F_T^I	−0.35	**0.89**	−0.30	**0.74**		**−0.89**	0.24	**0.96**	−0.26
	F_N^M	**0.97**	−0.03	**0.88**	0.33		**0.72**	0.30	0.06	**0.99**
	F_T^M	0.18	**0.94**	−0.34	**0.77**		**0.88**	0.38	**−0.82**	−0.35
1	F_N^I	**0.98**	−0.13	**0.93**	0.06	**7**	0.33	**0.92**	**0.95**	0.11
	F_T^I	−0.02	**0.78**	−0.06	**0.84**		**−0.93**	0.20	**0.93**	−0.33
	F_N^M	**0.97**	0.07	**0.86**	−0.30		**0.87**	0.25	0.03	**0.93**
	F_T^M	−0.03	**0.76**	−0.11	**0.80**		**0.92**	−0.38	**−0.93**	−0.15
2	F_N^I	**0.97**	0.05	0.10	**0.92**	**8**	−0.18	**0.97**	**0.88**	0.33
	F_T^I	−0.04	**−0.78**	−0.07	**0.92**		**−0.83**	0.30	**0.91**	0.39
	F_N^M	**0.95**	0.01	**0.92**	0.28		**0.89**	−0.01	−0.10	**0.97**
	F_T^M	−0.10	**0.80**	**−0.94**	0.23		**0.93**	−0.35	**−0.91**	−0.28
3	F_N^I	**−0.97**	−0.06	0.14	**0.90**	**9**	0.08	**0.99**	**0.88**	0.24
	F_T^I	**0.86**	0.14	−0.04	**0.96**		**−0.91**	−0.20	**0.98**	−0.26
	F_N^M	−0.07	**0.93**	**0.90**	−0.09		**0.87**	0.34	0.25	**0.98**
	F_T^M	0.38	**0.80**	**−0.85**	−0.20		**0.95**	−0.29	**−0.93**	0.10
4	F_N^I	**0.90**	−0.25	0.05	**0.92**	**10**	−0.04	**0.99**	**0.66**	−0.30
	F_T^I	**−0.93**	0.03	−0.05	**0.98**		**−0.96**	0.13	**0.91**	−0.25
	F_N^M	0.02	**0.95**	**0.84**	−0.35		**0.97**	0.29	0.09	**0.96**
	F_T^M	0.27	**0.92**	**−0.86**	−0.33		**0.91**	−0.20	**-0.87**	−0.39
5	F_N^I	**0.93**	−0.10	−0.03	**0.92**					
	F_T^I	**−0.88**	−0.32	0.21	**0.93**					
	F_N^M	−0.03	**0.92**	**0.93**	−0.09					
	F_T^M	0.21	**0.93**	**−0.88**	−0.32					

Data are from a representative subject. F_N^I index normal force; F_T^I index tangential force; F_N^M middle normal force; F_T^M middle tangential force. Absolute values of the loadings over 0.7 are shown in bold.

middle fingers in the CW condition were grouped into PC1 and PC2, respectively, while these loading patterns were reversed in the CCW condition. Furthermore, the two tangential force components and the normal force which contribute to the antagonist moment (i.e., F_N^M in the CW, F_N^I in the CCW) were grouped into PC1, and the other normal force contributable to agonist moment was solely PC2 under relatively higher moment arm conditions (e.g., $6 \sim 10$ cm conditions).

Discussion

The current experiment produced both expected and unexpected outcomes; therefore, the hypotheses formulated in the introduction to this paper are partially supported. We observed a significant increase in the stability indices for all four PVs, including the resultant moment of force (M^{RES}), the moment of tangential force (M_T^{RES}), and the force direction (F_{DIR}) when the MA of the tangential force increased. This observation supported our second and third hypotheses. As the moment arm of the tangential force increased, conjoint changes in the normal forces were observed. However, given that the magnitudes of the tangential forces *decreased*, our first hypothesis was not fully supported.

Biomechanical Aspects of the Use of Mechanical Advantage

The human hand and fingers exemplify the motor redundancy that is observed at various levels of the human movement system. The redundancy implies that the number of variables (e.g., individual finger forces in the current study) that need to be organized is greater than the number of constraints that enforce the relationships among the variables (e.g., zero net torque by actions of four force components in the current study). Therefore, a family of solutions could equally satisfy the given motor tasks. Further, the organization of proper sharing and co-variation among the involved elements is necessary to resolve this problem of redundancy. The individual contributions of elements to the overall performance could be characterized by using the principle of MA. Our findings were not in line with previously

reported results that showed increased force magnitudes with larger moment arms. In other words, we observed that the magnitudes of the tangential finger force slightly *decreased* with the moment arms. This finding was in direct opposition to previous observations (Slota, Latash, et al., 2012; Slota, Suh, et al., 2012). However, the current results may support the validity of the principle of MA during the usage of the tangential forces because of the following reasons. In the current experiment, the magnitudes of the external torque—that were supposed to be compensated for by the moment of produced finger forces—were tightly constrained. Meanwhile, there were no constrained values for both tangential and normal forces, such as a gravity-free experimental setup, and no target net normal force values. The magnitudes of the net forces had no constrained values; therefore, the relative contribution of the individual finger forces to the required mechanics—that is, the constrained value of the net torque—was important for gauging the benefit of the MA. We clearly observed that the relatively large share of the moment of the tangential force (M_T^{RES} in Figure 3) to the net moment was accompanied by reductions in the contribution of the moment of normal force (M_N^{RES} in Figure 3) when the MA (i.e., moment arm) of the tangential force was increased. These results were associated with an increased ratio of tangential to normal forces (i.e., direction of the force vector, F_{DIR} in Figure 2). Note that the tangential forces of both the index and middle fingers produced the moment in the required direction (i.e., agonist moment). This is further supported by the result of the PCA, which showed large loadings of the two tangential forces in the same PC, along with a large loading of normal force for the antagonist moment, especially during relatively large moment arm conditions (>6 cm). By combining all these outcomes, a tangential force with a large MA might effectively satisfy the task mechanics by incrementally changing their contributions, and by demonstrating task-specific compensation for an anti-directional moment.

Another interesting finding was that the relative contributions of the moment, by the two force components, crossed at the 4–5 cm moment arm conditions, while the magnitudes of the two forces continued to decrease (i.e., $F_N^{RES} > F_T^{RES}$ from 4–5 cm). In the current experiment, the magnitudes of the moment arm (i.e., the MA) of the normal forces were fixed at 2 cm, and the friction coefficients between the fingertips and contact surface were approximately 1.40 and 1.52 (Zatsiorsky et al., 2003a). Again, there were no constrained values of either normal or tangential forces, unlike holding an object in the air (i.e., the sum of the digit tangential forces should compensate for the weight of the object being grasped in a static fashion). However, normal forces should be sufficient to maintain the rotational equilibrium given the friction coefficient. This means that the magnitudes of the tangential forces were partially constrained due to the friction mechanics. This may result in a relatively larger contribution of the normal force to the net moment at the 2 cm condition, where the MAs of the two force components were equal. Therefore, the patterns of force shares in this study comply with the principle of MA, and with the mechanical necessities of the given environment (i.e., the friction coefficient). As the moment of tangential force increased—as the MA increased—the contribution of normal forces to the net moment decreased to satisfy the constraint of having the same net torque for all experimental conditions. These variable patterns might also be modulated synergic actions of the finger forces, which incited the chain-effect observed in the current results.

Torque and Force Direction Stabilization with Mechanical Advantage

The stability of a given task is crucial for achieving functional actions by multiple elements in a redundant motor system (Latash, 2016; Zatsiorsky & Latash, 2008). We sought to determine if using the MA was beneficial for stabilizing salient PV(s), such as stabilization of net moment by purposeful co-variation of the four components of the finger forces. The stability index (ΔV) of the apparent PV (i.e., ΔV_M^{RES}) increased with the magnitudes of the tangential moment arms. Meanwhile, opposite changes between ΔV_M of normal (ΔV_M^N) and tangential forces (ΔV_M^T) showed a direct proportion for ΔV_M^T and an inverse proportion for ΔV_M^N relative to the magnitudes of the moment arm (Figure 4). Further, the force direction (ΔV_F^{DIR}, i.e., the angle of force vector) was also stabilized—and even strengthened—as the moment arms increased (Figure 6). To the best of our knowledge, this was the first experimental evidence of parallel changes in the stability indices with the magnitudes of MA for particular elements (i.e., tangential forces). The use of MA was associated with the beneficial consequence of the "*economy*" of total finger force production—as shown in previous studies (Park et al., 2012) and current results (i.e., the decrement in the force magnitudes and SM)—but also with the stabilization of net outcome variables that involved an abundant set of elements. Here, we deliberately use the term "*abundant*" rather than "*redundant*" because previous studies and current outcomes have shown that combinations of a redundant set of finger forces vary, not by freezing the element actions, but by covarying all the involved elements properly and stabilizing task mechanics. This study provides additional evidence of "*active*" control of a tangential force (Park et al., 2010; Shim & Park, 2007), and our results support the hypothesis that MA has a beneficial effect on fine-tuning (or trial-to-trial tuning) of a set of four force components. Indeed, the analysis of the stability index and the dimension reduction

(i.e., PCA) showed that inter-trial tuning to stabilize the net moment created two subsets where the configurations underwent conjoint adjustments as the moment arms increased. For small moment arm conditions (e.g., 0–2 cm), decoupled subsets of normal and tangential forces were observed. These results were similar to prior findings that supported the principle of superposition (Shim et al., 2005b; Shim & Park, 2007; Zatsiorsky et al., 2004).

However, we hesitate to claim that the current results (i.e., decoupled control of normal and tangential forces) support the validity of superposition control. This is because both subsets contribute to the generation and stabilization of the net moment. In other words, the two subsets are not separable elements of functional performance, such as grasping and rotational equilibrium. This is particularly evident during static prismatic grasping (Ambike et al., 2013; Zatsiorsky et al., 2004). Again, there were no constrained values or tasks for pressing forces or tangential forces in the current experiment. Our interpretation of the existence of the two subsets during small moment arm conditions was that the fine-tuning of tangential forces was not coupled with normal force tuning. This implies that the tangential force might consist of independent force components that are controlled during finger force generation (i.e., active control of the tangential force). Similarly, two independent subsets of the force components were still observed at larger moment arm conditions, while the configurations of the subsets were modulated as the moment arms increased. Functionally, the first subset seemed to compensate for the anti-directional moment of force produced by one of the normal forces. Here, we observed large loadings of two tangential forces with one normal force in the same PC. Note that the tangential forces produced by the two fingers always produced the moment of force in the required direction (i.e., agonist moment production). Meanwhile, one of the normal forces produced the anti-directional moment of force due to the geometry of the experimental frame and the task mechanics. In addition, the variance explained by the first two PCs increased, while the variance within the task space (i.e., the UCM space) decreased with the moment arms. These results imply that first, the planarity of data distributions was stronger when a relatively large MA was used. Second, less-flexible finger force combinations were associated with better stability due to smaller error variances (V_{ORT}). Note that the strength of stability properties (i.e., synergy index) reflects the relative amounts of variances of UCM space (V_{UCM}) to its orthogonal space (V_{ORT}) with respect to the total variance (V_{TOT}). Thus, it is possible that lower V_{UCM} is compatible with either higher or lower synergy indices depending on the relative amounts of the two variances (Kapur et al., 2010; Kim et al., 2018). Hence, finger force combinations with relatively large MAs may be nearly optimal combinations within a two-dimensional hyperplane (i.e., such combinations would be more likely to comply with the optimal principle, *see* Terekhov et al., 2010; Terekhov & Zatsiorsky, 2011) without sacrificing stability. Then, what is the nature of the cost-function implemented in the current data set? Despite the fact that the magnitudes of finger force and SM decreased with the moment arms in the current results, the force magnitude-related variables may not be the cost to be minimized due to the observation of the antagonist moment production. Instead, the current results of the increased stability index (i.e., synergy index) with more converged finger force combination (i.e., smaller variance) infer that the cost to be minimized may not be "energy" because the system could not reproduce robust stability during the conservation of energy (Ahn & Hogan, 2012). A true cost-function implemented by the human controller may be related to the combinations of several human factors such as biomechanical, physiological, and psychological variables; thus, future research will have to ascertain the veracity of possible cost-function that actually implemented by the central nervous system.

During the current motor tasks, the finger force vectors were supposed to be observed in the frontal plane (y-z plane). This was caused by the actions of the fingers following the issuance of instructions that were associated with flexion and abduction/adduction using the distal interphalangeal (IP) and metacarpophalangeal (MCP) joints (Pataky et al., 2008). The tangential force (the abduction/adduction along the y-axis) was predominantly generated by activation of intrinsic hand muscles (e.g., the dorsal interosseous and the palmar interosseous) at the MCP joint (Li et al., 2003). Extrinsic hand muscles (e.g., the flexor digitorum superficialis and profundus) contributed to the flexion moment by generating normal force at the IP joint (Li et al., 2000). Since the current task required simultaneous production of y- and z-axis forces, the coordinated actions of the extrinsic and intrinsic muscles were critical to maintaining the stability of salient PVs. It seems that the two groups of muscles—intrinsic and extrinsic—stabilized the salient PVs by organizing the two independent subsets. This resulted in conjoint adjustments with changes in MA. Together, these produced incremental changes in the stability index for the net moment as the salient PV.

The elemental variables employed in the current analysis were finger forces in both the normal and tangential directions. Individual finger forces are interdependent due to biomechanical and neural structures in humans. This phenomenon is referred to as "enslaving" (Van Beek et al., 2019; Zatsiorsky et al., 2000). In the current analysis, our justification was that the enslaving patterns of tangential force production were more complex than those of normal forces (Pataky et al., 2007). Further, the

particular relations between the interdependency of normal and tangential forces has not been discovered yet. The actions of the index and middle fingers, which were the fingers involved in the current experiment, function relatively independently compared to other fingers. Therefore, we focused on force variability and its effect on performance using a set of mechanical variables (i.e., finger forces).

The main result of our study is the demonstration that the tangential forces actively utilized the given MA for the moment of force production, which supported the validity of the principle of MA during the finger tangential force production. In particular, the principle of MA can be beneficial not only for efficient force production but also for stabilization of PVs by proper co-variation of an abundant set of elements. Nevertheless, we have to admit the limitations of the current study such as the nature of current task. Since the simultaneous stabilizations of grasping and rotational equilibrium are required in many everyday activities, future studies will have to determine whether the current conclusion would be reached during more ecologically valid tasks.

Disclosure statement

No potential conflict of interest was reported by the author(s).

Funding

This work was supported in part by the Ministry of Science and the National Research Foundation of Korea (NRF-2019R1F1A1061871), the Creative-Pioneering Researchers Program through Seoul National University (SNU), and Nano·Material Technology Development Program through the National Research Foundation of Korea (NRF) funded by the Ministry of Science, ICT and Future Planning (No. 2016M3A7B4910552).

REFERENCE

Adams, S. K., & Peterson, P. J. (1988). Maximum voluntary hand grip torque for circular electrical connectors. *Human Factors*, *30*(6), 733–745. https://doi.org/10.1177/001872088803000609

Ahn, J., & Hogan, N. (2012). A simple state-determined model reproduces entrainment and phase-locking of human walking. *PLoS One*, 7(11), e47963. https://doi.org/ARTNe4796310.1371/journal.pone.0047963 https://doi.org/10.1371/journal.pone.0047963

Ambike, S. S., Paclet, F., Latash, M. L., & Zatsiorsky, V. M. (2013). Grip-force modulation in multi-finger prehension during wrist flexion and extension. *Experimental Brain Research*, *227*(4), 509–522. https://doi.org/10.1007/s00221-013-3527-z

Biewener, A. A., Farley, C. T., Roberts, T. J., & Temaner, M. (2004). Muscle mechanical advantage of human walking and running: Implications for energy cost. *Journal of Applied Physiology*, *97*(6), 2266–2274. https://doi.org/10.1152/japplphysiol.00003.2004

Buchanan, T. S., Rovai, G. P., & Rymer, W. Z. (1989). Strategies for muscle activation during isometric torque generation at the human elbow. *Journal of Neurophysiology*, *62*(6), 1201–1212. https://doi.org/10.1152/jn.1989.62.6.1201

Demircan, E., Yung, S., Choi, M., Baschshi, J., Nguyen, B., & Rodriguez, J. (2020). Operational space analysis of human muscular effort in robot assisted reaching tasks. *Robotics and Autonomous Systems*, *125,* 103429. https://doi.org/10342910.1016/j.robot.2020.103429 https://doi.org/10.1016/j.robot.2020.103429

Devlin, H., & Wastell, D. G. (1986). The mechanical advantage of biting with the posterior teeth. *Journal of Oral Rehabilitation*, *13*(6), 607–610. https://doi.org/10.1111/j.1365-2842.1986.tb00684.x

Flanagan, J. R., & Wing, A. M. (1993). Modulation of grip force with load force during point-to-point arm movements. *Experimental Brain Research*, 95(1), 131–143.

Johansson, R. S., & Westling, G. (1984). Roles of glabrous skin receptors and sensorimotor memory in automatic-control of precision grip when lifting rougher or more slippery objects. *Experimental Brain Research*, 56(3), 550–564.

Kaiser, H. F. (1960). The application of electronic-computers to factor-analysis. *Educational and Psychological Measurement*, *20*(1), 141–151. https://doi.org/10.1177/001316446002000116

Kapur, S., Zatsiorsky, V. M., & Latash, M. L. (2010). Age-related changes in the control of finger force vectors. *Journal of Applied Physiology*, 109(6), 1827–1841. https://doi.org/10.1152/japplphysiol.00430.2010

Kim, K., Xu, D. Y., & Park, J. (2018). Effect of kinetic degrees of freedom on multi-finger synergies and task performance during force production and release tasks. *Scientific Reports*, 8, 12758. https://doi.org/10.1038/s41598-018-31136-8

Kuo, A. D. (1994). A mechanical analysis of force distribution between redundant, multiple degree-of-freedom actuators in the human - implications for the central-nervous-system. *Human Movement Science*, 13(5), 635–663. https://doi.org/10.1016/0167-9457(94)90010-8

Latash, M. L. (2012). The bliss (not the problem) of motor abundance (not redundancy). *Experimental Brain Research*, *217*(1), 1–5. https://doi.org/10.1007/s00221-012-3000-4

Latash, M. L. (2016). Towards physics of neural processes and behavior. *Neuroscience and Biobehavioral Reviews*, *69*, 136–146. https://doi.org/10.1016/j.neubiorev.2016.08.005

Latash, M. L., Scholz, J. P., & Schoner, G. (2007). Toward a new theory of motor synergies. *Motor Control*, *11*(3), 276–308. https://doi.org/10.1123/mcj.11.3.276

Latash, M. L., Shim, J. K., Gao, F., & Zatsiorsky, V. M. (2004). Rotational equilibrium during multi-digit pressing and prehension. *Motor Control*, *8*(4), 392–404. https://doi.org/10.1123/mcj.8.4.392

Li, Z. M., Pfaeffle, H. J., Sotereanos, D. G., Goitz, R. J., & Woo, S. L. Y. (2003). Multi-directional strength and force envelope of the index finger. *Clinical Biomechanics*, *18*(10), 908–915. https://doi.org/10.1016/S0268-0033(03)00178-5

Li, Z. M., Zatsiorsky, V. M., & Latash, M. L. (2000). Contribution of the extrinsic and intrinsic hand muscles to

the moments in finger joints. *Clinical Biomechanics*, *15*(3), 203–211. https://doi.org/10.1016/S0268-0033(99)00058-3

Martin, J. R., Latash, M. L., & Zatsiorsky, V. M. (2011). Coordination of contact forces during multifinger static prehension. *Journal of Applied Biomechanics*, *27*(2), 87–98. https://doi.org/10.1123/jab.27.2.87

Nichols, T. R. (1994). A biomechanical perspective on spinal mechanisms of coordinated muscular action: An architecture principle. *Acta Anatomica*, *151*(1), 1–13. https://doi.org/10.1159/000147637

Oldfield, R. C. (1971). The assessment and analysis of handedness: The Edinburgh inventory. *Neuropsychologia*, *9*(1), 97–113. https://doi.org/10.1016/0028-3932(71)90067-4 https://doi.org/10.1016/0028-3932(71)90067-4

Park, J., Baum, B. S., Kim, Y. S., Kim, Y. H., & Shim, J. K. (2012). Prehension synergy: Use of mechanical advantage during multifinger torque production on mechanically fixed and free objects. *Journal of Applied Biomechanics*, *28*(3), 284–290. https://doi.org/10.1123/jab.28.3.284

Park, J., Han, D. W., & Shim, J. K. (2015). Effect of resistance training of the wrist joint muscles on multi-digit coordination. *Perceptual and Motor Skills*, 120(3), 816–840. https://doi.org/10.2466/25.26.PMS.120v16x9

Park, J., Kim, Y. S., & Shim, J. K. (2010). Prehension synergy: Effects of static constraints on multi-finger prehension. *Human Movement Science*, *29*(1), 19–34. https://doi.org/10.1016/j.humov.2009.11.001

Pataky, T. C., Latash, M. L., & Zatsiorsky, V. M. (2004). Tangential load sharing among fingers during prehension. *Ergonomics*, *47*(8), 876–889. https://doi.org/10.1080/00140130410001670381

Pataky, T. C., Latash, M. L., & Zatsiorsky, V. M. (2007). Finger interaction during maximal radial and ulnar deviation efforts: Experimental data and linear neural network modeling. *Experimental Brain Research*, *179*(2), 301–312. https://doi.org/10.1007/s00221-006-0787-x

Pataky, T. C., Latash, M. L., & Zatsiorsky, V. M. (2008). Multifinger Ab- and adduction strength and coordination. *Journal of Hand Therapy*, *21*(4), 377–385. https://doi.org/10.1197/j.jht.2008.02.002

Pheasant, S., & O'Neill, D. (1975). Performance in gripping and turning -a study in hand/handle effectiveness. *Applied Ergonomics*, *6*(4), 205–208. https://doi.org/10.1016/0003-6870(75)90111-8

Prilutsky, B. I. (2000). Coordination of two- and one-joint muscles: Functional consequences and implications for motor control. *Motor Control*, *4*(1), 1–373. https://doi.org/10.1123/mcj.4.1.1

Reschechtko, S., Zatsiorsky, V. M., & Latash, M. L. (2015). Task-specific stability of multifinger steady-state action. *Journal of Motor Behavior*, *47*(5), 365–377. https://doi.org/10.1080/00222895.2014.996281

Scholz, J. P., Danion, F., Latash, M. L., & Schoner, G. (2002). Understanding finger coordination through analysis of the structure of force variability. *Biological Cybernetics*, *86*(1), 29–39. https://doi.org/10.1007/s004220100279

Scholz, J. P., & Schoner, G. (1999). The uncontrolled manifold concept: Identifying control variables for a functional task. *Experimental Brain Research*, *126*(3), 289–306. https://doi.org/10.1007/s002210050738

Shim, J. K., Latash, M. L., & Zatsiorsky, V. M. (2003). Prehension synergies: Trial-to-trial variability and hierarchical organization of stable performance. *Experimental Brain Research*, 152(2), 173–184. https://doi.org/10.1007/s00221-003-1527-0

Shim, J. K., Latash, M. L., & Zatsiorsky, V. M. (2004). Finger coordination during moment production on a mechanically fixed object. *Experimental Brain Research*, *157*(4), 457–467. https://doi.org/10.1007/s00221-004-1859-4

Shim, J. K., Latash, M. L., & Zatsiorsky, V. M. (2005a). Prehension synergies in three dimensions. *Journal of Neurophysiology*, *93*(2), 766–776. https://doi.org/10.1152/jn.00764.2004

Shim, J. K., Latash, M. L., & Zatsiorsky, V. M. (2005b). Prehension synergies: Trial-to-trial variability and principle of superposition during static prehension in three dimensions. *Journal of Neurophysiology*, *93*(6), 3649–3658. https://doi.org/10.1152/jn.01262.2004

Shim, J. K., Park, J., Zatsiorsky, V. M., & Latash, M. L. (2006). Adjustments of prehension synergies in response to self-triggered and experimenter-triggered load and torque perturbations. *Experimental Brain Research*, 175(4), 641–653. https://doi.org/10.1007/s00221-006-0583-7

Shim, J. K., & Park, J. B. (2007). Prehension synergies: Principle of superposition and hierarchical organization in circular object prehension. *Experimental Brain Research*, *180*(3), 541–556. https://doi.org/10.1007/s00221-007-0872-9

Slota, G. P., Latash, M. L., & Zatsiorsky, V. M. (2012). Tangential finger forces use mechanical advantage during static grasping. *Journal of Applied Biomechanics*, *28*(1), 78–84. https://doi.org/10.1123/jab.28.1.78

Slota, G. P., Suh, M. S., Latash, M. L., & Zatsiorsky, V. M. (2012). Stability control of grasping objects with different locations of center of mass and rotational inertia. *Journal of Motor Behavior*, *44*(3), 169–178. https://doi.org/10.1080/00222895.2012.665101

Terekhov, A. V., Pesin, Y. B., Niu, X., Latash, M. L., & Zatsiorsky, V. M. (2010). An analytical approach to the problem of inverse optimization with additive objective functions: An application to human prehension. *Journal of Mathematical Biology*, *61*(3), 423–453. https://doi.org/10.1007/s00285-009-0306-3

Terekhov, A. V., & Zatsiorsky, V. M. (2011). Analytical and numerical analysis of inverse optimization problems: Conditions of uniqueness and computational methods. *Biological Cybernetics*, *104*(1–2), 75–93. https://doi.org/10.1007/s00422-011-0421-2

Throckmorton, G. S., & Dean, J. S. (1994). The relationship between Jaw-muscle mechanical advantage and activity levels during isometric bites in humans. *Archives of Oral Biology*, *39*(5), 429–437. https://doi.org/10.1016/0003-9969(94)90174-0

Todorov, E., Li, W. W., & Pan, X. C. (2005). From task parameters to motor synergies: A hierarchical framework for approximately optimal control of redundant manipulators. *Journal of Robotic Systems*, *22*(11), 691–710. https://doi.org/10.1002/rob.20093

Van Beek, N., Stegeman, D. F., Jonkers, I., de Korte, C. L., Veeger, D., & Maas, H. (2019). Single finger movements in the aging hand: Changes in finger independence, muscle

activation patterns and tendon displacement in older adults. *Experimental Brain Research*, *237*(5), 1141–1154. https://doi.org/10.1007/s00221-019-05487-1

Zatsiorsky, V. M., Gao, F., & Latash, M. L. (2003a). Finger force vectors in multi-finger prehension. *Journal of Biomechanics*, *36*(11), 1745–1749. https://doi.org/10.1016/S0021-9290(03)00062-9

Zatsiorsky, V. M., Gao, F., & Latash, M. L. (2003b). Prehension synergies: Effects of object geometry and prescribed torques. *Experimental Brain Research*, *148*(1), 77–87. https://doi.org/10.1007/s00221-002-1278-3

Zatsiorsky, V. M., Gregory, R. W., & Latash, M. L. (2002a). Force and torque production in static multifinger prehension: Biomechanics and control. I. Biomechanics. *Biological Cybernetics*, *87*(1), 50–57. https://doi.org/10.1007/s00422-002-0321-6

Zatsiorsky, V. M., Gregory, R. W., & Latash, M. L. (2002b). Force and torque production in static multifinger prehension: Biomechanics and control. II. Control. *Biological Cybernetics*, *87*(1), 40–49. https://doi.org/10.1007/s00422-002-0320-7

Zatsiorsky, V. M., & Latash, M. L. (2008). Multifinger prehension: An overview. *Journal of Motor Behavior*, *40*(5), 446–475. https://doi.org/10.3200/JMBR.40.5.446-476

Zatsiorsky, V. M., Latash, M. L., Gao, F., & Shim, J. K. (2004). The principle of superposition in human prehension. *Robotica*, *22*, 231–234. https://doi.org/10.1017/S0263574703005344

Zatsiorsky, V. M., Li, Z. M., & Latash, M. L. (2000). Enslaving effects in multi-finger force production. *Experimental Brain Research*, *131*(2), 187–195. https://doi.org/10.1007/s002219900261

Received April 5, 2020
Revised August 10, 2020
Accepted August 13, 2020